



# Microfluidic doublets in aqueous samples generated by microfabricated thermal probes

Amar S. Basu<sup>\*</sup>, Yogesh B. Gianchandani<sup>1</sup>

Department of Electrical Engineering and Computer Science, University of Michigan, United States

## ARTICLE INFO

### Article history:

Received 27 July 2009

Received in revised form

25 November 2009

Accepted 8 December 2009

Available online 16 December 2009

### Keywords:

Doublet  
Thermal probe  
Thermal gradient  
Marangoni flow  
Surface tension  
Particle manipulation  
Vortex

## ABSTRACT

This paper describes an investigation of microfluidic actuation of doublet patterns in samples of water on blank substrates, using singular and arrayed microfabricated thermal probes. A doublet is a two-dimensional flow pattern consisting of adjacent, opposing vortices with linear streamlines between them. In this work, each probe consists of a polyimide thin film cantilever with a metal heater near the tip which generates a temperature gradient up to  $1\text{ }^\circ\text{C}/\mu\text{m}$  along its length. The probes are  $360\text{ }\mu\text{m}$  long,  $42\text{--}120\text{ }\mu\text{m}$  wide, and  $3.5\text{ }\mu\text{m}$  thick, and the tips are typically  $<1\text{ mm}$  away from the liquid surface. The velocity of the doublet flow can be controlled by adjusting the temperature of the heat source or by controlling the gap or attack angle between the heat source and the liquid surface. Linear flow velocities exceeding  $5\text{ mm/s}$  and rotational velocities exceeding  $1200\text{ rpm}$  are reported.

© 2009 Elsevier B.V. All rights reserved.

## 1. Introduction

The ability to manipulate particles is important in several types of biological assays, most notably those involving cells, biomolecules, and bead supports for solid-phase chemistry. Mechanisms for manipulating particle solutions generally fall into two categories: (1) forces which act directly on the particles, and (2) forces imparted on the particles by microflow patterns in the surrounding fluid. The first category includes methods such as optical tweezers [1], dielectrophoresis [2], and optically induced dielectrophoresis [3]. Each of these methods relies on the dielectric properties of the particle. In contrast, the second class of methods is largely independent of the particle's material properties, relying instead on the interaction of the particle with the surrounding fluid. Many of these methods work by generating vortices which trap the particles in a recirculating flow. Microflow patterns can be acoustically generated using out-of-plane [4] or in-plane piezoelectric transducers [5]. When operated at or near the res-

onant frequency (typically several  $100\text{ kHz}$ ), the actuators create ultrasonic standing waves which can trap microscale beads and other particles. Due to the challenges in fabricating mechanical components in planar fabrication processes [6], non-mechanical techniques have also been investigated. For example, an opto-electrostatically driven vortex generated by a focused  $50\text{ mW}$  laser spot in combination with a  $2\text{ kV/cm}$  electric field was shown to provide a maximum particle velocity of  $120\text{ }\mu\text{m/s}$  in conductive liquids [7]. Vortices driven by electrokinetic instability formed in polymer channels with patterned surface charges [8] operate on a smaller electric field ( $100\text{ V/cm}$ ), but produce slower velocities and require ionic solutions [9]. Pressure differentials and dielectrophoresis [10] are other active methods for generating vortices for particle manipulation.

The Marangoni effect refers to flow on a liquid surface in the presence of surface tension gradients. Due to the inverse relation between surface tension and temperature, Marangoni flow patterns can be deliberately formed by imposing a temperature gradient on the surface [11]. Past approaches have used miniature heaters of various geometries suspended above the fluid layer to generate flow patterns [12,13] in thin layers of oil. In this work, a microfabricated cantilever probe with a sharp linear temperature gradient is used to drive a unique doublet flow in thin films of water.<sup>2</sup>

<sup>\*</sup> Corresponding author. Present address: Electrical and Computer Engineering Department, Wayne State University, 5050 Anthony Wayne Drive, Detroit, MI 48202, United States. Tel.: +1 313 577 3990.

E-mail addresses: [abasu@eng.wayne.edu](mailto:abasu@eng.wayne.edu), [basua@umich.edu](mailto:basua@umich.edu) (A.S. Basu), [yogesh@umich.edu](mailto:yogesh@umich.edu) (Y.B. Gianchandani).

<sup>1</sup> Present address: Department of Electrical Engineering and Computer Science, University of Michigan, 1301 Beal Avenue, Ann Arbor, MI 48109-2122, United States. Tel.: +1 734 615 6407.

<sup>2</sup> Portions of this work appear in conference abstract form in [14].

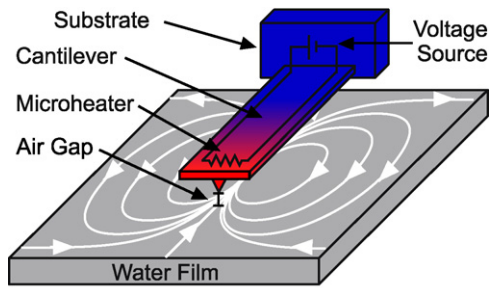


**Fig. 1.** Schematic of doublet flow generation. A heated thermal probe suspended above a film of water induces a high-speed doublet flow pattern at the surface. The color gradient along the length of the cantilever probe represents a temperature gradient that forms across the cantilever when a current is passed through the microheater.

A fluidic doublet is a two-dimensional flow pattern with streamlines analogous to the field lines in an electric or magnetic dipole. Although rarely observed in nature, doublets can be realized by placing a fluidic sink and source adjacent to one another. Such extraction/injection well pairs have been implemented at very large scales because their mixing characteristics can efficiently purify groundwater [15,16]. Evans [17] and Cola [18] implemented source-sink pairs in microfabricated devices to facilitate advective mixing. A mixing chamber was flanked by channels which either pumped fluid away or into the chamber in a pulsatile fashion. Efficient mixing was demonstrated; however, the devices require mechanical actuation, provided by either integrated [17] or off-chip components [18].

Here, we present experimental evidence that a high speed fluidic doublet, with rotational velocities exceeding 1200 rpm and linear velocities of 5 mm/s, can be realized on a thin aqueous layer placed on a glass slide, without a fluidic chip or pumps. The doublet is driven by a thermal probe suspended above the liquid surface (Fig. 1). Since the probe has no moving parts and makes no contact with the liquid, common problems of mechanical wear, electrode contamination, and bubble generation can be avoided. Additionally, the technique is not restricted to ionic or conductive liquids.

Section 2 introduces the doublet and briefly describes a theoretical model. Section 3 gives experimental results of a typical doublet, and also describes how multiple heat sources (i.e., a thermal probe array) can be superimposed to generate uniform flow.

## 2. Theoretical

As mentioned above, the doublet is a two-dimensional potential flow consisting of two adjacent vortices of opposing rotational directions, and resulting linear streamlines between them (Fig. 1). It can be expressed in Cartesian coordinates ( $x, y$ ) by its stream function  $\psi_D$  [19]:

$$\psi_D \approx \frac{ma}{\pi} \frac{y}{x^2 + y^2 - a^2} \quad (1)$$

Here,  $m$  is a constant, and  $2a$  is the separation between the two poles. The product  $ma$ , also called the dipole moment, reflects the strength of the doublet. The doublet stream function is related to its velocity vector ( $u, v$ ) as:

$$u = \frac{d\psi}{dy} = \frac{ma}{\pi} \left( \frac{x^2 - y^2}{(x^2 + y^2 - a^2)^2} \right) \quad (2)$$

$$v = -\frac{d\psi}{dx} = \frac{ma}{\pi} \left( \frac{2xy}{(x^2 + y^2 - a^2)^2} \right) \quad (3)$$

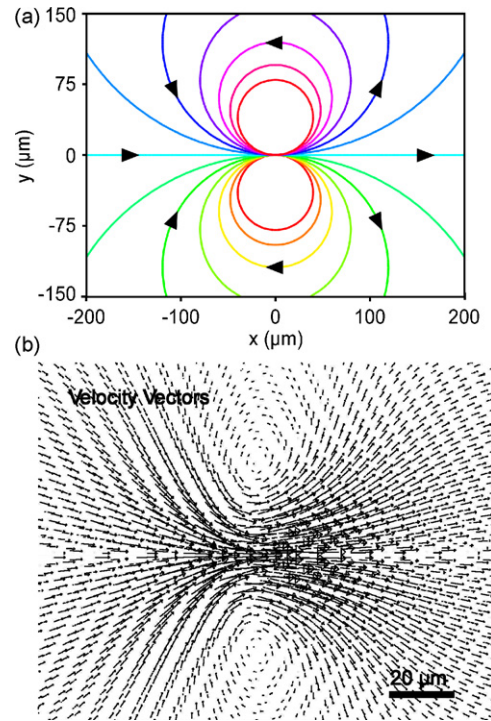


**Fig. 2.** Analytical and numerical modeling results for a doublet. (a) Theoretical stream function of an ideal doublet with dipole moment  $25 \times 10^{-6} \text{ m}^3/\text{s}$ , (b) CFD simulation of doublet flow due to surface momentum  $10^{18} \text{ kg m/s per m}^2$  applied to a  $20 \mu\text{m} \times 20 \mu\text{m}$  region in a two-dimensional fluid layer. The maximum surface velocity vector in this simulation is  $200 \text{ mm/s}$ .

Fig. 2a illustrates the streamlines for a typical doublet with a dipole moment  $25 \times 10^{-6} \text{ m}^3/\text{s}$ , which is relevant to the experimental observations described in Section 3.

One way that a doublet flow pattern can be generated on a liquid surface is by adding momentum to a small region on the fluid surface. This is shown in simulations using commercial CFD software (Fluent 6.0, Fluent Corp.). A two-dimensional fluid layer with dimensions  $300 \mu\text{m} \times 300 \mu\text{m}$  is meshed with  $2 \mu\text{m}$  square elements, and a linear momentum of  $10^{18} \text{ kg m/s per m}^2$  is applied to a  $20 \mu\text{m} \times 20 \mu\text{m}$  region in the center of the fluid layer. Under these conditions, doublet flow is observed with scale and geometry similar to the analytical solution above (Fig. 2b). The surface velocity is highest at the center of the doublet, with a maximum velocity of  $200 \mu\text{m/s}$ .

Localized momentum can be imparted to the surface of a liquid via the Marangoni effect. If a directional temperature gradient is imposed on the liquid interface, a corresponding surface tension gradient is also formed due to the inverse relation between surface tension and temperature. Surface stresses result in Marangoni flow oriented from the warm to the cool regions [11,12]. In a typical thermal probe with length  $250 \mu\text{m}$ , a temperature gradient up to  $1^\circ\text{C}/\mu\text{m}$  can be formed along the length of the cantilever. If the probe is positioned near the liquid surface, the temperature gradient is transferred to the surface. Fig. 3 illustrates simulation results where a  $360 \mu\text{m} \times 120 \mu\text{m} \times 3 \mu\text{m}$  probe with a  $7 \mu\text{m}$  tall pyramidal tip is suspended  $15 \mu\text{m}$  above a stationary liquid layer. The sharp, asymmetric gradient produced on the liquid surface (Fig. 3b), which can be controlled by the attack angle of the probe, offers a cause for the forward doublets oriented from the left to right.

## 3. Experimental

The microfabricated thermal probe consists of a thin film cantilever with a joule heater on the distal end. The probe is fabricated

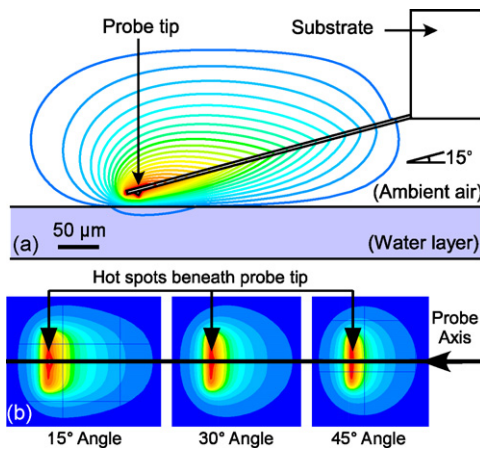


**Fig. 3.** (a) Cross-section of a three-dimensional thermal simulation showing a cantilever probe held 15 μm above the liquid surface. There are 20 equally spaced contours between 306 and 300 K, which is the ambient temperature. (b) Top view of the temperature profile on the liquid surface for 3 different probe attack angles. The maximum surface temperature increase is 0.3 K.

in a 6-step surface micromachining process in which the polyimide cantilever and metal layers are formed on a substrate, released, and subsequently flipped over so that the probe overhangs the silicon substrate [20]. The same process can be used to make a multi-probe array [21]. In this work, two probe geometries are used: R01 (length 360 μm, width 42 μm, resistance 25–40 Ω), and R02 (length 360 μm, width 120 μm, resistance 20–35 Ω). The probe tip can be heated to 250 °C with <20 mW input power. When heated, a sharp temperature gradient is formed along the length of the probe.

Fig. 4 shows the doublet flow resulting from a thermal probe suspended approximately 20 μm above the surface of a thin water layer with 15 mW input power. (The air gap between the tip and the sample presents a very large thermal resistance, as noted previously and illustrated in Fig. 3.) Deionized water was spread on a glass slide to the desired depths, typically 50–100 μm. Due to the evaporation of the water films, the typical duration of the experiments was kept to <10 min. If desired, film evaporation can be minimized by increasing the ambient humidity. Polystyrene beads (diameter 3–10 μm, Polysciences) were immersed in the water to serve as tracer particles. The time-sequence micrographs, taken at

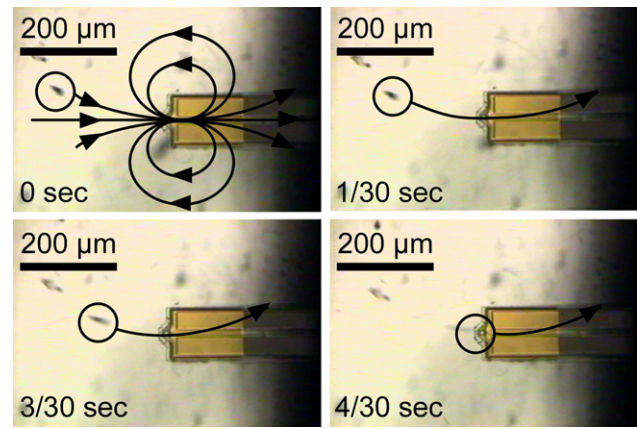


**Fig. 4.** High-speed doublet flow is illustrated in 4 sequential micrographs taken at 1/30 s intervals. Polystyrene beads are used to visualize the flow.

1/30 s intervals with a CCD camera, show the movement of the tracers in a high speed, symmetric doublet flow. The maximum flow velocity, measured just to the left of the probe tip, was found to be ~5 mm/s. The streamlines and velocities are similar to the analytical model (Fig. 2) which assumes the two poles have a separation  $2a = 10 \mu\text{m}$  and have a strength  $m = 5 \times 10^{-6} \text{ m}^2/\text{s}$ . Based on this, the approximate dipole moment of the experimentally measured doublet is  $25 \times 10^{-6} \text{ m}^3/\text{s}$ .

The linear relationship between input power and flow velocity is shown in Fig. 5a. For example, with the cantilever held at a fixed 25 μm gap above the liquid surface, flow velocities increase by approximately 90 μm/s for every 1 mW applied, up to a maximum power of 32 mW. Since it is known that the tip temperature increases linearly with input power [20], results show that the flow is proportional to tip temperature.

Reducing the air gap between the probe and the water surface permits the same flow velocities to be achieved at lower levels of input power. For example, extrapolating the results in Fig. 5a suggests that at a 25 μm gap, one can obtain 5000 μm/s surface flow velocity by applying 55 mW power to the probe. At a 10 μm gap, the same velocity can be obtained with only 10 mW power (Fig. 5b). Flow velocities decrease roughly as the inverse square of the air gap. The maximum recorded experimental velocities were obtained at

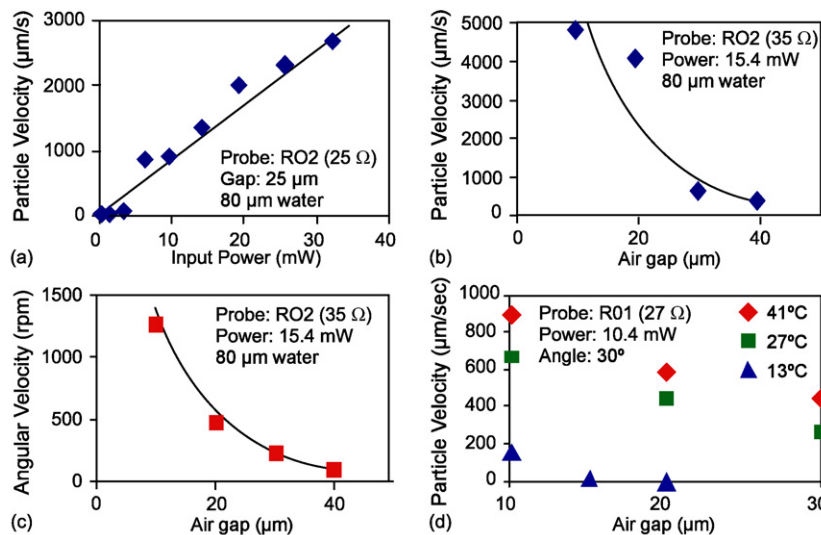


**Fig. 5.** Control of flow velocities. (a and b) Peak linear flow velocity as a function of (a) input power, and (b) air gap. (c) Rotation rate in the vortices, as a function of air gap. (d) Flow velocity vs. air gap repeated for three different ambient liquid temperatures. Experimental conditions are shown in each plot. The lines in (a) are a linear fit, and the lines in (b and c) are a fit to  $1/x^2$ .

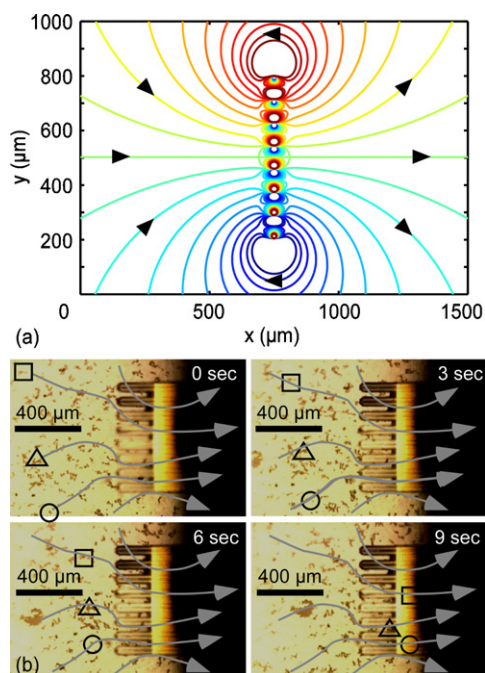


**Fig. 6.** Uniform flow generated with a linear array of doublets. (a) Theoretical streamlines of flow generated by an array of 8 doublets with  $85\ \mu\text{m}$  spacing, obtained by summing the respective stream functions. (b) Linear flow generation using an 8-probe array, numbered 1–8 from the top down. The array was placed  $15\text{--}20\ \mu\text{m}$  above the liquid surface, held at a  $15^\circ$  angle, and biased with a total power of  $92\ \text{mW}$ . Probes 1 and 4 were nonfunctional. Trajectories for 3 particles are marked with a square, triangle, and circle on micrographs taken at 3 s intervals.

air gaps of  $<10\ \mu\text{m}$ . Linear velocities of  $5000\ \mu\text{m/s}$  (Fig. 5b) and rotational velocities of  $1200\ \text{rpm}$  (Fig. 5c) in the adjacent vortices were obtained with  $15\ \text{mW}$  input power to the probe.

Liquid temperature also plays an important role in determining flow velocities. Cooled liquids generally have larger viscosity and smaller temperature gradients, both of which will reduce Marangoni flow velocities [13]. Fig. 5d shows the consequence of biasing the glass slide below the water sample at  $13$ ,  $27$ , and  $41^\circ\text{C}$  using a circulating heating/cooling plate. At each temperature, particle velocities were measured as a function of air gap while holding the probe at constant power and angle. Trends of faster velocities with smaller air gaps hold true as before, but higher liquid temperatures shift the entire trend upward. For example, at a  $\approx 10\ \mu\text{m}$  air gap, the particle velocity at  $13^\circ\text{C}$  is only  $165\ \mu\text{m/s}$ , compared to nearly  $900\ \mu\text{m/s}$  at  $41^\circ\text{C}$ . Overall, particle velocities shown in this figure are slower than the results shown in Fig. 5b due to lower input power levels and the fact that a thinner probe (R01) was used, both of which reduce the surface heat flux.

Complex flow patterns can be generated by forming arrays of doublets using multiple thermal sources. In order to predict the theoretical flow pattern which would arise from multiple doublets, the stream equations for each doublet may be added by applying the principle of superposition. For example, the flow pattern generated by a linear array of 8 doublets with  $85\ \mu\text{m}$  spacing is shown in Fig. 6a. This particular geometry was chosen to model the structure of the multiprobe array. The flow pattern, which resembles a uniform flow channel, was confirmed in experiments. An array of 8 thermal probes [21] was biased at  $2.3\ \text{V}$ , dissipating  $92\ \text{mW}$  total power in six probes (probes 1 and 4 were nonfunctional). The resulting flow pattern has a linear flow region with adjacent rotational regions as predicted by simulations (Fig. 6b).

Deviations from uniform flow that were observed in several regions, such as the trajectory marked with a triangle, can be attributed to the difference in air gap between the various probes

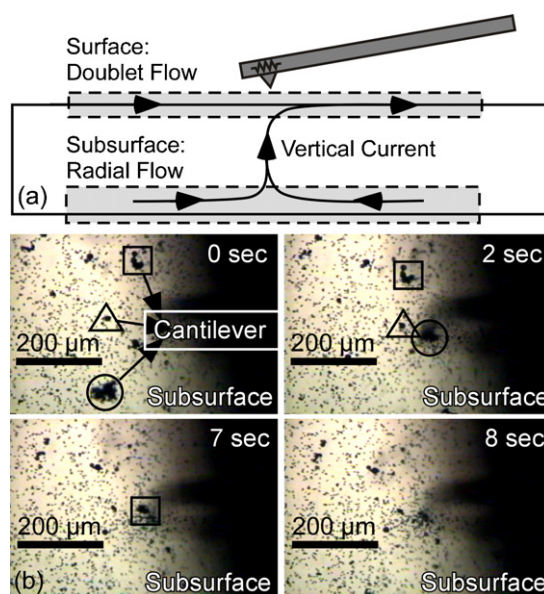


**Fig. 7.** (a) Schematic of subsurface particle flow ( $80\ \mu\text{m}$  below the surface). Particles flow radially inward towards the area underneath the microheater tip. Upon reaching this point, they are immediately propelled upwards to the surface. (b) Sequential micrographs show three particles (marked respectively with a square, triangle, and circle) converge towards the center and then disappear from the field of view as they are propelled upwards.

in the array, and the fact that two probes were not operational. The noticeably smaller velocities ( $190\ \mu\text{m/s}$ ) compared to single probes may be attributed to the smaller temperatures of the heaters in the multiprobe array compared to the single probe. These results illustrate that flow is highly dependent on the geometry of the heat transmitted to the liquid surface. Therefore, it is possible to obtain custom flow patterns by arranging the heat sources in various configurations.

Subsurface particle flow, visualized by focusing the microscope at the bottom of an  $80\ \mu\text{m}$  thick layer of water, differs significantly from the doublet flow patterns observed at the surface. Particles flow radially inward over time, converging on a point directly below the tip of the cantilever. Once at this point, the particles are accelerated upwards toward the surface of the liquid layer (Fig. 7).

#### 4. Discussion and conclusions

This effort has evaluated the doublet flow patterns that are established in films of water when a microfabricated thermal probe is used as the heating element. Linear flow velocities of  $5000\ \mu\text{m/s}$  and rotational velocities up to  $1200\ \text{rpm}$  are demonstrated using a microfabricated probe at a  $10\text{--}20\ \mu\text{m}$  gap and  $<20\ \text{mW}$  input power to the probe. Higher velocities can theoretically be achieved with higher input power to the probe.

The doublet flow pattern can be modeled by local momentum added to the fluid. The momentum, in turn, can be the result of Marangoni stresses caused by a temperature profile imposed on the liquid surface. A directional temperature gradient supplied by the probe evidently leads to the formation of a doublet flow pattern. Although this work has focused on the thermal probes designed in our laboratory [20,21], our results suggest that theoretically, any cantilever structure with a sharp thermal gradient could generate doublet flow. It is notable that a symmetrical, needle-like probe oriented above the water will not produce doublet flow; the asymmetry appears to play an important role in the directionality of flow. There is also some indication that flow direction can be reversed under certain conditions when the probe angle is large.

The tendency of water to evaporate may additionally play a role in doublet formation, as the doublet flow pattern is only observed in water, and not in nonvolatile media such as mineral oil. In the long term, models that simultaneously evaluate localized evaporation and Marangoni stresses may help to fully elucidate the microflow patterns. On the experimental side, studies with more complex probe shapes and materials may reveal additional possibilities for this non-contact method of fluidic actuation.

### Acknowledgements

The authors thank Dr. Shamus McNamara for assistance in probe fabrication. Support was provided in part by the National Science Foundation, the University of Michigan, and a Whitaker Foundation Biomedical Engineering Fellowship (A.S.B.). Y. Gianchandani acknowledges support through the IR/D program while working at the National Science Foundation. The findings do not necessarily reflect the views of the NSF.

### References

- [1] A. Ashkin, Optical trapping and manipulation of neutral particles using lasers, *Proc. Natl. Acad. Sci. U.S.A.* 94 (1997) 4853.
- [2] S. Fiedler, S.G. Shirley, T. Schnelle, G. Fuhr, Dielectrophoretic sorting of particles and cells in a microsystem, *Anal. Chem.* 70 (1998) 1909–1915.
- [3] P.Y. Chiou, A.T. Ohta, M.C. Wu, Massively parallel manipulation of single cells and microparticles using optical images, *Nature* 436 (2005) 370–372.
- [4] T. Kajiyama, H. Tomita, Y. Miyahara, Manipulation of micro air bubbles in a flow through cell using ultrasonic standing waves, in: *Proc. Intl. Conference on Solid-State Sensors and Actuators (Transducers)*, 1999, pp. 764–767.
- [5] G.M. Dougherty, A.P. Pisano, Ultrasonic particle manipulation in microchannels using phased co-planar transducers, in: *Proc. Intl. Conference on Solid-State Sensors, Actuators and Microsystems (Transducers)*, 2003, pp. 670–673.
- [6] Y. Gianchandani, O. Tabata, H. Zappe, *Comprehensive Microsystems*, Elsevier Science and Technology, Cambridge, 2007.
- [7] A. Mizuno, M. Nishioka, Y. Ohno, L. Dascallescu, Liquid micro-vortex generated around a laser focal point in an intense high-frequency electric field, in: *Conference Record IAS Annual Meeting*, 1993, pp. 1774–1778.
- [8] M.H. Oddy, J.G. Santiago, J.C. Mikkelsen, Electrokinetic instability micromixing, *Anal. Chem.* 73 (Dec 2001) 5822–5832.
- [9] W.L.W. Hau, L.M. Lee, Y.K. Lee, M. Wong, Y. Zohar, Experimental investigation of electrokinetically generated in-plane vorticity in a microchannel, in: *Proc. Intl. Conference on Solid-State Sensors Actuators and Microsystems (Transducers)*, 2003, pp. 651–654.
- [10] Y.-K. Lee, J. Deval, P. Tabeling, C.-H. Ho, Chaotic mixing in electrokinetically and pressure driven micro flows, in: *Proc. IEEE International Conference on Micro Electro Mechanical Systems (MEMS)*, 2001, pp. 483–486.
- [11] A.S. Basu, Y.B. Gianchandani, Shaping high-speed marangoni flow in liquid films by microscale perturbations in surface temperature, *Appl. Phys. Lett.* 90 (2007) 03410/1–03410-3.
- [12] A.S. Basu, Y.B. Gianchandani, Virtual microfluidic traps, filters, channels and pumps using Marangoni flows, *J. Micromech. Microeng.* 18 (2008) 115031.
- [13] A.S. Basu, Y.B. Gianchandani, A Programmable Array for Contact-Free Manipulation of Floating Droplets on Featureless Substrates by the Modulation of Surface Tension, *Journal of Microelectromechanical Systems* 18 (2009) 1163–1172.
- [14] A.S. Basu, Y.B. Gianchandani, High speed microfluidic doublet flow in open pools driven by non-contact micromachined thermal sources, in: *Proc. IEEE International Conference on Micro Electro Mechanical Systems (MEMS)*, 2005, pp. 666–669.
- [15] J. Luo, P.K. Kitanidis, Fluid residence times within a recirculation zone created by an extraction–injection well pair, *J. Hydrol.* 295 (August) (2004) 149–162.
- [16] R.K. Gandhi, G.D. Hopkins, M.N. Goltz, S.M. Gorelick, P.L. McCarty, Full-scale demonstration of in-situ cometabolic biodegradation of trichloroethylene in groundwater, 1: dynamics of a recirculating well system, *Water Resources Research* 38 (April) (2002) 10.1–10.16.
- [17] J. Evans, D. Liepmann, A.P. Pisano, Planar laminar mixer, in: *Proc. IEEE International Conference on Micro Electro Mechanical Systems (MEMS)*, 1997, pp. 96–101.
- [18] B.A. Cola, D.K. Schaffer, T.S. Fisher, M.A. Stremler, A pulsed source-sink fluid mixing device, *J. Microelectromech. Syst.* 15 (February) (2006) 259–266.
- [19] D.F. Young, B.R. Munson, T.H. Okiishi, W. Heebisch, *A Brief Introduction to Fluid Mechanics*, Wiley, New York, 2007.
- [20] M.H. Li, Y.B. Gianchandani, Applications of a low contact force polyimide shank bolometer probe for chemical and biological diagnostics, *Sens. Actuators A: Phys.* 104 (May 2003) 236–245.
- [21] S. McNamara, A.S. Basu, Y.B. Gianchandani, Ultracompliant thermal probe arrays, *J. Micromech. Microeng.* 15 (January) (2004) 237–243.

### Biographies



**Amar S. Basu** received the BSE and MSE degrees in electrical engineering in 2001 and 2003, the MS degree in biomedical engineering in 2005, and the Ph.D. degree in electrical engineering in 2008, all with honors from the University of Michigan, Ann Arbor. He has worked with Intel's Advanced Technology Division, General Motors, and Silicon Graphics, and served as an adjunct faculty at the electrical engineering department at the University of Michigan. Currently, he is an assistant professor at the electrical and computer engineering department at Wayne State University, where he is developing micro and nanoscale systems for high throughput screening and other areas of biological research.

Dr. Basu was a recipient of the Whitaker Foundation Biomedical Engineering Fellowship in 2003, and was voted the IEEE Professor of the Year by the student body in 2009. His work as a consultant with Mobius Microsystems and Picocal has resulted in a number of US patents.



**Yogesh B. Gianchandani** received a B.S., M.S., a Ph.D. in electrical engineering, with a focus on microelectronics and MEMS. He is presently a Professor at the University of Michigan, Ann Arbor, with a primary appointment in the Electrical Engineering and Computer Science Department and a courtesy appointment in the Mechanical Engineering Department. He also serves as the Deputy Director for the Center for Wireless Integrated Microsystems (WIMS).

Dr. Gianchandani's research interests include all aspects of design, fabrication, and packaging of micromachined sensors and actuators and their interface circuits (<http://www.eecs.umich.edu/~yogesh/>). He has published more than 200 papers in journals and conferences, and has about 30 US patents issued or pending. He was a Chief Co-Editor of *Comprehensive Microsystems: Fundamentals, Technology, and Applications*, published in 2008. He serves several journals as an editor or a member of the editorial board, and served as a General Co-Chair for the IEEE/ASME International Conference on Micro Electro Mechanical Systems (MEMS) in 2002. From 2007 to 2009 he also served at the National Science Foundation, as the program director for Micro and Nano Systems within the Electrical, Communication, and Cyber Systems Division (ECCS). Dr. Gianchandani is a Fellow of IEEE.